ELSEVIER Thermochimica Acta 275 (1996) 37-49

thermochimica acta

Thermal behaviour of cotton–modacrylic fibre blends: kinetic study using the invariant kinetic parameters method

Laurence Richard-Campisi [a,b], Serge Bourbigot [a,*], Michel Le Bras [a], René Delobel [b]

[a] *Laboratoire de Physicochimie des Solides, E.N.S.C.L, Université des Sciences et Technologies de Lille, BP 108, F-59652 Villeneuve d'Ascq Cedex, France*

[b] *Centre de Recherche et d'Etude sur les Procédés d'Ignifugation des Matériaux (C.R.E.P.I.M.), BP 49, F-62160 Bully les Mines, France*

Received 22 May 1995; accepted 5 September 1995

Abstract

This work studies the thermooxidative degradation of cotton and modacrylic fabrics and of a cotton–modacrylic blend. The association in a blend of modacrylic with cotton fibres is used to improve the fire behaviour of the latter. Using the IKP method which allows the degradation of the material to be modelled, we demonstrate that better thermal stability does not imply better fire-proofing properties, but that these are controlled by the fuel flow rate feeding the flame.

Keywords: Cotton–modacrylic blend; Fabrics; Fire behaviour; IKP method

1. Introduction

Textile materials, and in particular cotton-based fabrics, are inflammable and it is necessary to develop successful flame-retardant systems or blends of textile fibres to prevent fire hazards [1].

In this laboratory, we study blends of cotton-based fibres [2, 3] which may impart flame-retardant properties to the fabrics. In particular the association of modacrylic fibres (synthetic polymeric product) with cotton fabrics (natural polymeric product) in a blend provides fire-proofing properties of interest (Table 1). It is interesting to note that the evaluation of the ignitability of the material with a match suggests a synergistic phenomenon.

---

[*] Corresponding author.

SSDI 0040-6031(95)02729-7

Table 1
Evaluation of fire-proofing properties using several normalized tests of cotton-based fabrics

Material	LOI[a] %	Cigarette[b]	Match[c] in s	Flame spread in 45°[d] cm s^{-1}
Cotton	18.4	0	5	1.75
Modacrylic	32.3	1	15	0
Cotton–Modacrylic	24.0	1	20	0.72

[a] Limiting Oxygen Index [4].
[b] Evaluation of the ignitability by smoker's materials of upholstered composites for seating with a cigarette [5].
[c] As preceding, with a match [6].
[d] Measurement of flame spread of 45° oriented specimens [7].

The burning process depends on chemical processes occurring in the bulk of the polymeric materials (condensed phase) and above the material surface (gas phase), and also on the physical process of heat transfer from the gas phase back to the condensed phase. All three of these depend primarily on the thermal degradation reactions in the condensed phase, which generate volatile products and may also change the physical character of the surface of the sample [8].

This paper deals with a thermal degradation kinetic study (using the IKP method, see the Appendix) of a cotton–modacrylic blend fabric in order to understand its fire behaviour in comparision with single-fibre fabrics [9–11]. First, the degradations of cotton and modacrylic fabrics were studied in order to compare them independently and then the blend was investigated in order to understand interactions between the cotton and the modacrylic and its fire behaviour.

2. Experimental

2.1. Materials

Cotton fibres (cotton) investigated are derived from cellulose-based seeds of the cotton plant (gossypium) (woven by the Institut Textile de France). Modacrylic fibres are linear macromolecules formed from 50–80 wt% of the acrylonitrile unit and from 50–20 wt% of the vinyl chloride unit, supplied by Rhovyl. Cotton–modacrylic fabrics (20 wt% cotton, 80 wt% modacrylic) were woven by Gratry-Lorthiois. Fig. 1 shows that the studied sample may not be considered as a homogeneous sample (cotton picks (warp) and modacrylic ends (weft)).

2.2. Thermal analysis

Thermogravimetric analyses were carried out at five heating rates ($\beta_v = 4, 5, 8, 10, 13$°C min^{-1}) under synthetic air (flow rate, 5×10^{-7} m^3/s^{-1}, Air Liquide grade) using

Fig. 1. SEM photography of the cotton–modacrylic blend fabric.

a Setaram MTB 10-8 microbalance. In each case the mass of sample used was fixed at 15 mg and the samples (fragments of the fabrics and not mixtures of the fibres) were positioned in open vitreous silica pans. The precision of the temperature measurement was 1.5°C in the whole of the range.

Computations of the invariant kinetic parameters and of the probabilities of the degradation functions were carried out using software developed in our laboratory (using the method described in the Appendix).

3. Results and discussion

3.1. Thermal degradation

The TG curves of the cotton fabrics (Fig. 2(a)), modacrylic fibres (Fig. 2(b)) and cotton–modacrylic blends (Fig. 2(c)) show two significant changes in their slopes, which indicate that the degradations are two-step processes. The first step may be assigned to the thermooxidative degradation of the fabrics which are transformed into carbonaceous residues. These latter may decompose during the second step of the degradation process.

In the case of the degradation of the cotton–modacrylic blend at $\beta_v = 4°\mathrm{C\ min}^{-1}$, an additional step appears between the first and second steps. The first step may be the superposition of the two degradations of the single components. This argument is confirmed by the temperature ranges which lie between 200 and 350°C and which correspond to the superposed temperature ranges of the first degradation steps of the

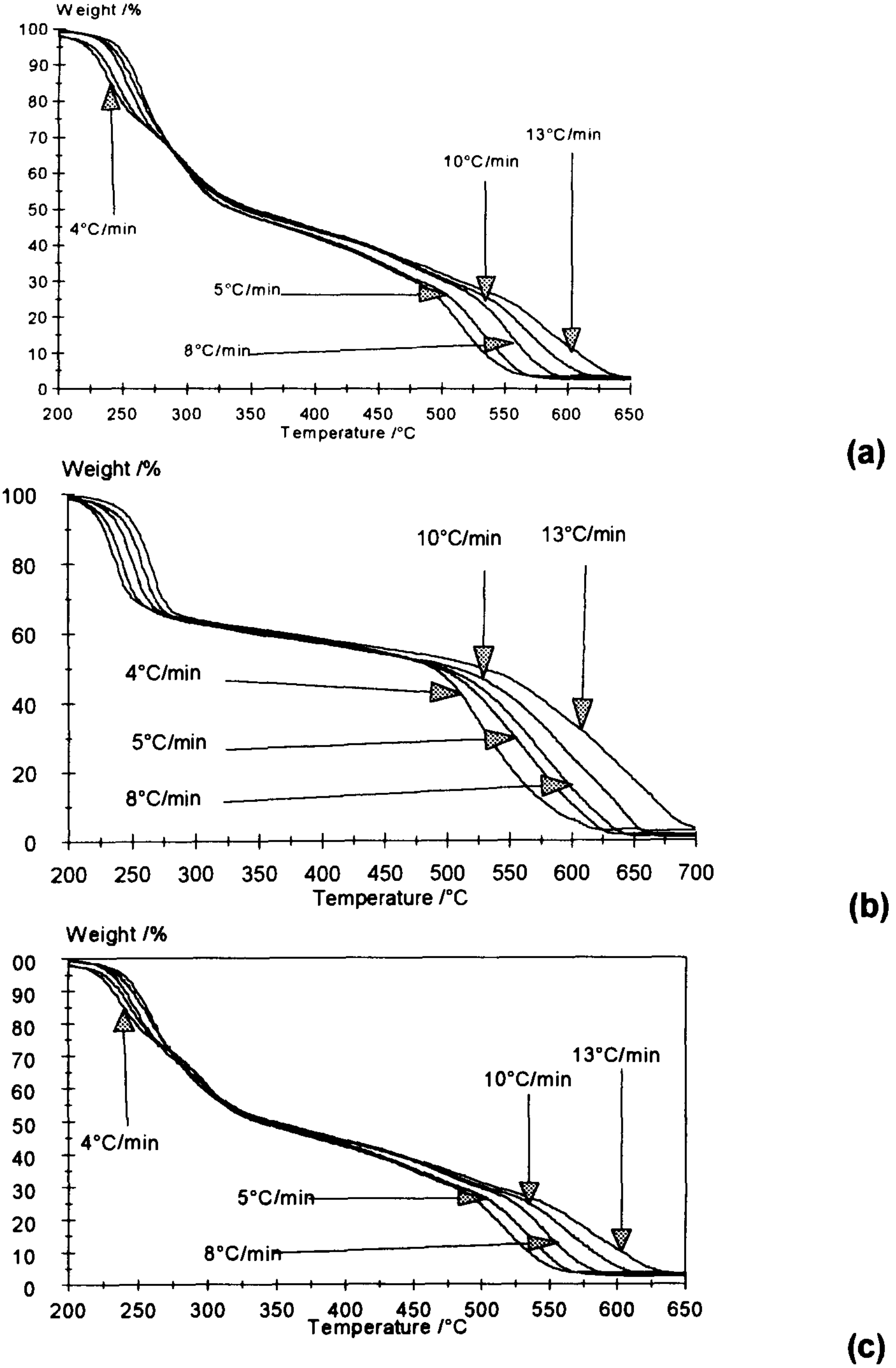

Fig. 2. TG curves of cotton fabric (a), modacrylic fibre (b) and cotton–modacrylic blend (c) at five heating rates.

single components. Furthermore, the weight loss (equal to 50% in the first step) corresponds to the linear combination of the weight losses of both components.

3.2. Computation of the invariant activation energy and pre-exponential factor

We studied only the first step of the degradation using the IKP method because we previously demonstrated that it may be related to the fire behaviour of the material [10,11].

The compensation effect is observed for each heating rate in each case (Fig. 3). The values of k_v at temperature T_v are then calculated from the slopes and intercepts of these above straight lines (Table 2).

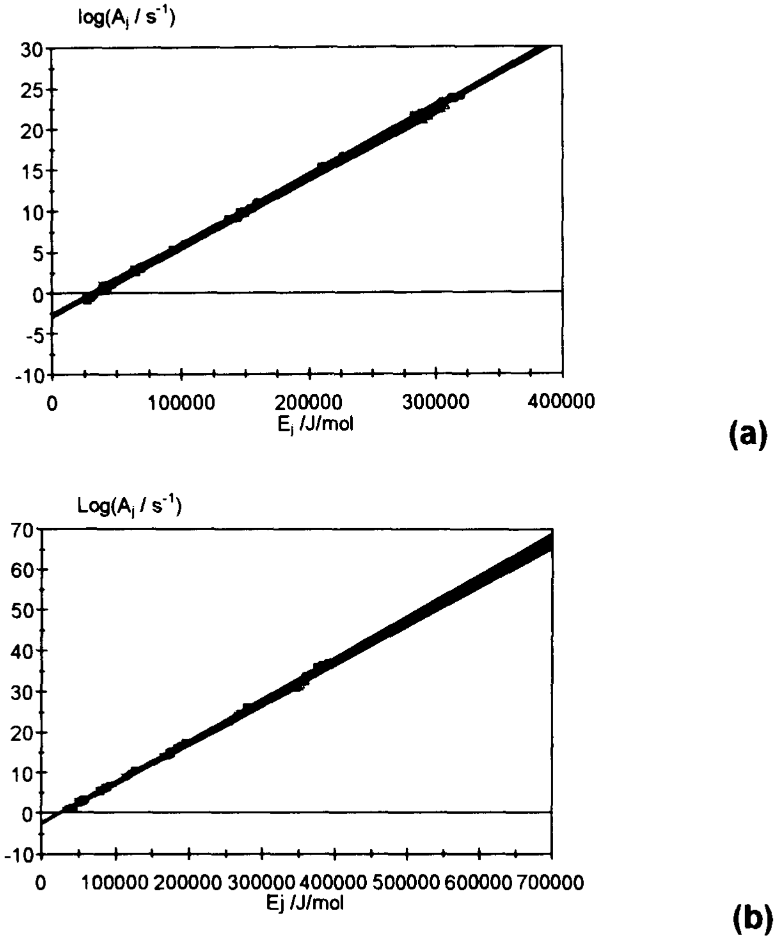

Fig. 3. Compensation effect observed between apparent activation energy and pre-exponential factor of cotton fabric (a), modacrylic fibre (b) and cotton–modacrylic blend (c).

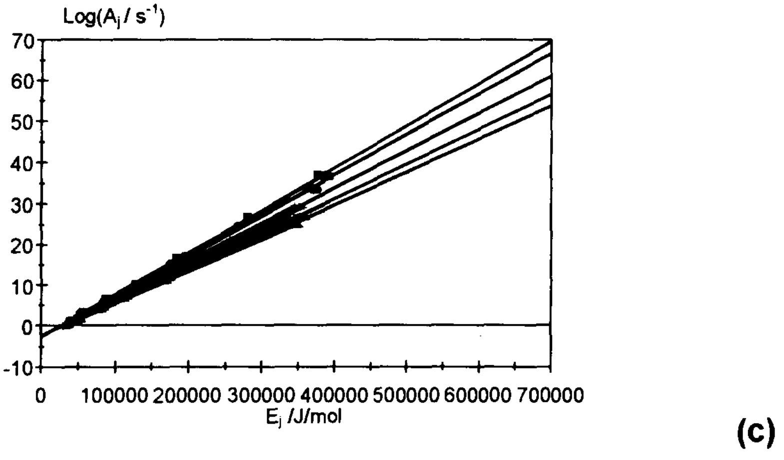

Fig. 3. (*Continued*)

Table 2
Rate constant k_v at temperature T_v computed from Fig. 3

Heating rate β_v/ °C $\min^{-1}$	$\log(k_v/s^{-1})$			T_v/°C		
	Cotton	Modacrylic	Cotton–Modacrylic	Cotton	Modacrylic	Cotton–Modacrylic
4	−2.9	−2.6	−2.7	336	240	246
5	−2.8	−2.5	−2.6	342	246	254
8	−2.6	−2.4	−2.5	351	255	265
10	−2.5	−2.3	−2.4	356	264	272
13	−2.4	−2.2	−2.3	362	269	278

A linear regression from the straight line plot of $\log k_v = \log A_{\mathrm{inv}} - (1/2.3RT_v) \times E_{\mathrm{inv}}$ allows computation of the invariant kinetic parameters (invariant pre-exponential factor A_{inv} and invariant activation energy E_{inv}) (Table 3).

The values computed for the cotton fabric are similar to those proposed by Faroq et al. [1] ($E = 155\ \mathrm{kJ\,mol^{-1}}$). The difference may be explained by the experimental conditions. Indeed, Faroq et al. worked under nitrogen flow and, therefore, studied the pyrolysis of the cotton fabric. Therefore, this means that the infuence of oxygen on the thermal stability of the cotton fabric is weak.

The thermal stability of the modacrylic fabric is lower than that of the cotton fabric, but the weight loss is only 40% during the first degradation step compared to 80% in the case of the cotton. This result shows that there is not the same relation observed in the case of unswollen polymers [12], i.e. the fire-proofing performances improve when the invariant activation energy increases [10,11]. This may be interpreted in terms of the nature of the gases evolved during the combustion, which are different, and/or as

Table 3
Invariant activation energies and pre-exponential factors of the cotton, modacrylic and cotton–modacrylic blend

Fabric	E_{inv}/kJ mol^{-1}	log A_{inv}/s^{-1}	r^2 [a]
Cotton	137	8.8	0.99
Modacrylic	77	5.2	0.99
Cotton–Modacrylic	56	3.0	0.99

[a] Regression coefficient.

the fuel flow rate which governs the degradation. Indeed a previous comparative study between the cotton and modacrylic fabrics using a fire model that can measure the rate of heat release (cone calorimeter [13]) has shown that the fuel flow evolved from the modacrylic and feeding the flame was less calorific than that of the cotton fabric [14].

The thermal stability of the modacrylic–cotton blend is lower than that of cotton and modacrylic fabrics but the fire-proofing performances are higher than those of the pure cotton fabric. As proposed above, this may be interpreted as being related to the nature of the evolved gases during the combustion of the blend and/or to a different fuel flow rate.

3.3. *Modellisation of the degradation*

The probability distributions are well discriminated (Fig. 4) and the degradation functions may be modelled by Eqs. (1)–(3) (Fig. 5)

$$f_{\mathrm{cotton}}(\alpha) = 0.1 \times 3 \times (1-\alpha)^{2/3} + 0.9 \times 3\alpha^{2/3} \quad (1)$$

$$f_{\mathrm{modacrylic}}(\alpha) = 0.02 \times 2(1-\alpha)[-\ln(1-\alpha)]^{1/2} + 0.4 \times 3(1-\alpha)[-\ln(1-\alpha)]^{2/3} + 0.58 \times 2\alpha^{1/2} \quad (2)$$

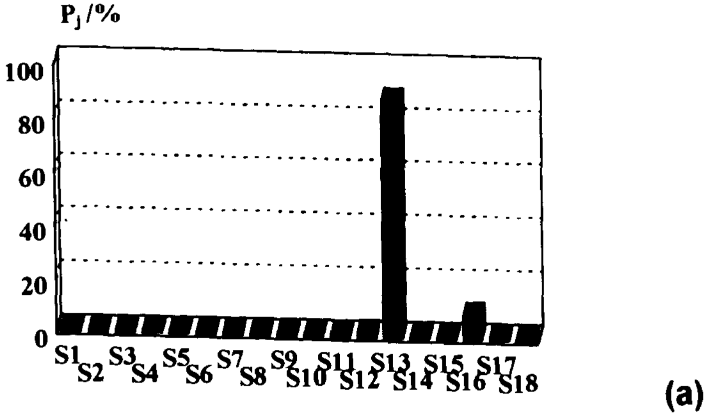

Fig. 4. Probabilities distribution of the kinetic degradation functions of cotton fabric (a), modacrylic fibre (b) and cotton–modacrylic blend (c).

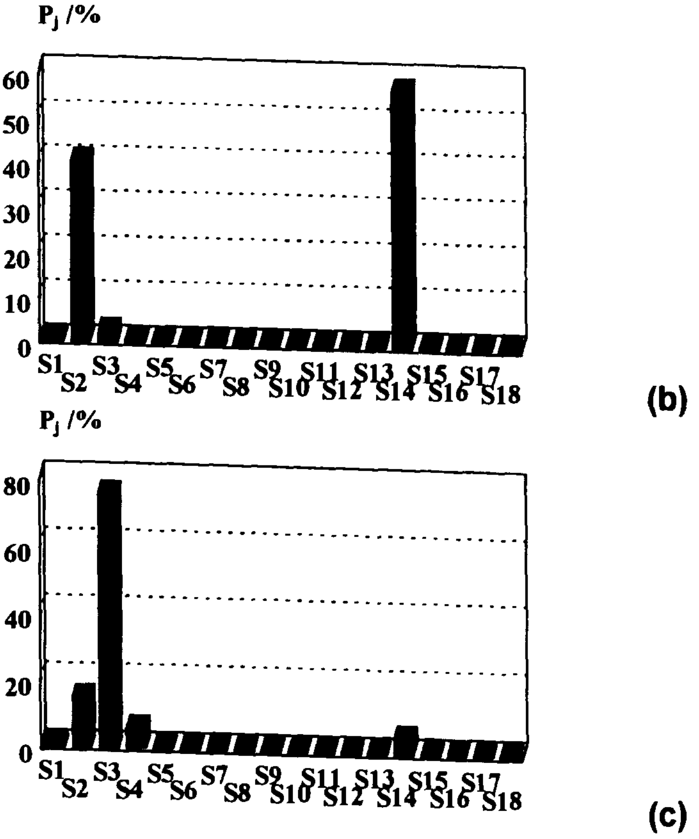

Fig. 4. (*Continued*)

$$\begin{aligned} f_{\mathrm{cotton/modacrylic}}(\alpha) = {} & 0.145 \times 3(1-\alpha)[-\ln(1-\alpha)]^{2/3} \\ & + 0.755 \times 2(1-\alpha)[-\ln(1-\alpha)]^{1/2} \\ & + 0.055 \times (3/2)(1-\alpha)[-\ln(1-\alpha)]^{1/3} + 0.045 \times 2\alpha^{1/2} \end{aligned} \quad (3)$$

It is observed that the modelled kinetic function of the cotton fabric increases when α increases (Fig. 5). This shows that the reaction of thermooxidative degradation autoaccelerates when α increases. This result should be compared with the function proposed by Faroq et al. [1] which was a second-order reaction. This function decreases when α increases which means that the pyrolysis of cotton fabric breaks when α increases. This comparison reveals the role of oxygen as a reactant in the thermal degradation of cotton fabrics.

The modelled kinetic function of the modacrylic fibres increases when α increases up to 0.7 and then decreases (Fig. 5). This shows, therefore, that the reaction of thermooxidative degradation first autoaccelerates and then breaks when α increases. This behaviour may explain the comparatively good fire-proofing properties by considering

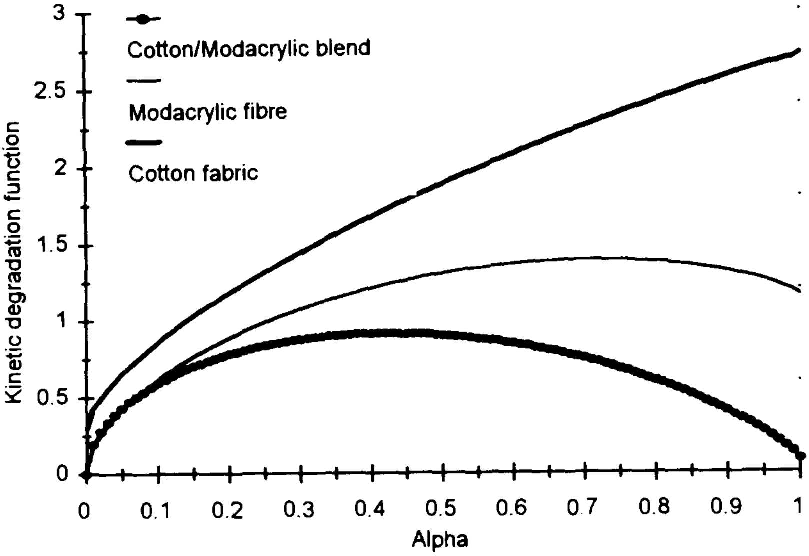

Fig. 5. Modelled degradation function of cotton fabric, modacrylic fibre and cotton–modacrylic blend versus α (see Eqs. (1)–(3)).

that the computed kinetic function models the fuel flow and by remarking that $f(\alpha)_{\mathrm{modacrylic}}$ is always lower than $f(\alpha)_{\mathrm{cotton}}$ whatever the α.

The probabilities distribution of the cotton–modacrylic blend shows that the degradation may be represented by a set of four probable kinetic functions. Moreover, this distribution suggests that the thermooxidative degradation of the blend represents not only the superimposed degradations of the single components, but also interactions and/or reactions between the modacrylic and the cotton during the degradation.

The resulting modelled kinetic function increases when α increases up to 0.4 and then decreases. This shows that the reaction of thermooxidative degradation first autoaccelerates and then breaks when α increases. This behaviour may explain the fire-proofing properties of cotton–modacrylic compared to those of cotton: $f(\alpha)_{\mathrm{cotton/modacrylic}}$ is always lower than $f(\alpha)_{\mathrm{cotton}}$. The better performances of the modacrylic fabric compared to that of the blend can be explained either by the better thermal stability of the fabric or by the nature of the evolved gases.

4. Conclusion

In this work, we have studied the thermooxidative degradation of cotton and modacrylic fabrics and of a cotton–modacrylic blend in order to explain the improvement in the fire behaviour of the cotton in a cotton–modacrylic blend. We have used the IKP method which models the degradation of the material. We have demonstrated that the best thermal stability did not imply the best fire-proofing properties: these were governed by the fuel flow rate feeding the flame and the nature of the gases evolved.

References

[1] A.A. Faroq, D. Price, G.J. Milnes and A.R. Horrocks, Polym. Deg. Stab., 44 (1994) 323.

[2] L. Richard, M. Brassard and R. Delobel, L'Industrie Textile, 1252 (1994) 37.

[3] L. Houillon and L. Richard, Techtextil Symp., 235 (1994) 1.

[4] Standard NF G 07-128, Détermination de l'indice d'oxygène à température ambiante.

[5] Standard ISO 8191-1, Assessment of the ease of ignition of upholstered seats—Ignition source: cigarette.

[6] Standard BS 5852, Assessment of the ease of ignition of upholstered seats—Ignition source: match equivalent flame.

[7] Standard NF G 07-182, Détermination des propriétés de propagation de flamme sur éprouvettes orientées à 45°.

[8] I.C. McNeill, Makromol. Chem., Makromol. Chem., Macromol. Symp., 74 (1993) 11.

[9] S. Bourbigot, R. Delobel, M. Le Bras and D. Normand, J. Chim. Phys., 90 (1993) 1909.

[10] S. Bourbigot, R. Delobel, M. Le Bras and Y. Schmidt, J. Chim. Phys., 89 (1992) 1835.

[11] R. Delobel, S. Bourbigot, M. Le Bras, Y. Schmidt and J.M. Leroy, Makromol. Chem., Macromol. Symp., 74 (1993) 59.

[12] H.L. Vandersall, J. Fire Flamm., 2 (1971) 97.

[13] V. Babraukas, Fire Mater., 8(2) (1984) 81.

[14] L. Richard-Campisi, Ph. D., University of Lille, 1995.

[15] A.I. Lesnikovich and S.V. Levchik, J. Therm. Anal., 27 (1983) 89.

[16] A.V. Nikoalev, V.A. Logvimenko and V.M. Gorberchev, J. Therm. Anal., 6 (1974) 473.

[17] A.W. Coats and J.P. Redfern, Nature, 201 (1964) 68.

[18] J.M. Criado and M. Gonzales, Thermochim. Acta, 46 (1981) 201.

[19] A.I. Lesnikovich, S.V. Levchik and V.G. Guslev, Thermochim. Acta, 77 (1984) 357.

[20] N. Koga and J. Sestak, J. Therm. Anal., 37 (1991) 1103.

[21] N. Koga, J. Sestak and J. Malek, Thermochim. Acta, 182 (1991) 333.

[22] J. Sestak, Thermophysical Properties of Solids, Elsevier, Amsterdam, 1984.

[23] N. Koga and J. Sestak, Thermochim. Acta, 182 (1991) 201.

[24] J. Malek, Thermochim. Acta, 200 (1992) 257.

[25] N. Koga, Thermochim. Acta, 244 (1994) 1.

[26] S. Bourbigot, R. Delobel, M. Le Bras and D. Normand, J. Chim. Phys., 90 (1993) 1909.

[27] P.G. Hoel, Statistique Mathématique, Armand Colin, Paris, 1991.

Appendix A

A.1. The invariant kinetic parameter method

In this method, several kinetic laws (18 functions $f_j(\alpha)$) indexed in Table A1 [15, 16] and different heating rates β_v are used. We assume only that the rate expression $\mathrm{d}\alpha/\mathrm{d}t$, where α is the degree of conversion, can be defined (as in isothermal conditions) by the equation

$$\mathrm{d}\alpha/\mathrm{d}t = kf(\alpha) \tag{A1}$$

and that the rate constant k follows the Arrhenius law

$$k = A\exp(-E/RT) \tag{A2}$$

Table A1
Kinetic models used

Kinetic models	$f_j(\alpha)$	$g_j(\alpha)$	
Nucleation and nucleus growing	$\frac{1}{n}(1-\alpha)(-\ln(1-\alpha))^{1-n}$	$(-\ln(1-\alpha))^n$	S1, $n = 1/4$
			S2, $n = 1/3$
			S3, $n = 1/2$
			S4, $n = 2/3$
			S5, $n = 1$
Phase boundary reaction	$(1-\alpha)^n$	$1-(1-\alpha)$	S6, plane symmetry
		$2[1-(1-\alpha)^{1/2}]$	S7, cylindrical symmetry
		$3[1-(1-\alpha)^{1/3}]$	S8, spherical symmetry
Diffusion	$\frac{1}{2}\alpha^{-1}$	α^2	S9, plane symmetry
	$(-\ln(1-\alpha))^{-1}$	$(1-\alpha)\ln(1-\alpha)+\alpha$	S10, cylindrical symmetry
	$\frac{3}{2}[(1-\alpha)^{-1/3}-1]^{-1}$	$1-\frac{2}{3}\alpha-(1-\alpha)^{2/3}$	S11, spherical symmetry
	$\frac{3}{2}(1-\alpha)^{1/3}[(1-\alpha)^{-1/3}-1]^{-1}$	$[(1-\alpha)^{1/3}-1]^2$	S18, Jander's type
Potential law	$\frac{1}{n}\alpha^{1-n}$	$\alpha^n (0 < n < 2)$	S12, $n = 1/4$
			S13, $n = 1/3$
			S14, $n = 1/2$
			S17, $n = 3/2$
Reaction order	$\frac{1}{n}(1-\alpha)^{1-n}$	$1-(1-\alpha)^{1/2}$	S15, $n = 1/2$
		$1-(1-\alpha)^{1/3}$	S16, $n = 1/3$

The eighteen apparent activation energies (E_{jv}) and pre-exponential factors (A_{jv}) are determined by the Coats and Redfern method [17] using the equation

$$\log\left(\frac{g_j(\alpha_{iv})}{T_{iv}^2}\right) = \log\left(\frac{A_{jv}R}{\beta_v E_{jv}}\right) - \frac{E_{jv}}{2.3RT_{iv}} \quad \text{with} \quad g_j(\alpha) = \int_0^{\alpha} \frac{d\alpha}{f_j(\alpha)} \tag{A3}$$

By plotting $\log(g_j(\alpha_{iv})/(T_{iv}^2)$ versus $1/T_{iv}$, the apparent activation energy E_{jv} and the apparent pre-exponential factor A_{jv} may be obtained.

The application of the IKP method is based on the study of the compensation effect (CE) [16,18]. For each function $f_j(\alpha)$, $\log A_j$ versus E_j is plotted and if a compensation effect is observed, a linear relation defined by the equation

$$\log A_{jv} = B_v + I_v E_{jv}$$

is obtained for each heating rate β_v [19]. A CE of this kind is classified as a false or superficial CE [20] resulting from parameter distortion by an inappropriate kinetic model function [21].

The significance of B_v and l_v has been discussed by Lesnikovich et al. [19] and it has been demonstrated that

$$B_v = \log(k_v)$$

$$l_v = \frac{1}{2.3RT_v} \tag{A4}$$

where k_v is the invariant rate constant of the system at the temperature T_v, these two parameters being characteristics of the experimental conditions. In this step, the isokinetic hypothesis, i.e. the invariant kinetic model function at different heating rates, is assumed [22,23]. Furthermore, the validity of these assumptions may be verified by the methods proposed by Malek [24] or Koga [25].

The essence of the method is to obtain a range of lines by varying the experimental conditions and to find the coordinates of its centre, i.e. E_{inv} and A_{inv} (invariant activation energy and pre-exponential factor). The coordinates are in an ellipsoidal domain that may be defined by the straight line [15]

$$B_v = \log \mathrm{A}_{\text{inv}} - E_{\text{inv}} l_v \tag{A5}$$

A.2. Probabilities of the kinetic degradation functions [26]

The kinetic functions $f_j(\alpha)$ may then be discriminated using the $\log A_{\text{inv}}$ and E_{inv} values obtained. Knowing n of the ith experimental values of $(\mathrm{d}\alpha/\mathrm{d}T)_{iv}$, the residual sum of squares for each $f_j(\alpha)$ and for each heating rate β_v may be computed

$$(n-1)Sj_{jv}^2 = \sum_{i=1}^{i=n} \left| \left(\frac{\mathrm{d}\alpha}{\mathrm{d}T}\right)_{iv} - \frac{A_{\text{inv}}}{\beta_v} \exp\left(-\frac{E_{\text{inv}}}{RT_{iv}}\right) f_j(\alpha_{iv}) \right|^2 \tag{A6}$$

The most probable function is then chosen by the average minimum value of $\bar{S}_j$ defined by the Eq. A7.

$$\bar{S}_j = \frac{1}{p} \sum_{v=1}^{v=p} S_{jv} \tag{A7}$$

with p the number of heating rates used.

The probability associated with each $f_j(\alpha)$ can be calculated by defining the equation

$$F_j = \frac{\bar{S}_j^2}{\bar{S}_{\min}^2} \tag{A8}$$

where $\bar{S}_j^2 = (1/pv)(\Sigma_{v=1}^{v=p} \bar{S}_{jv}^2)$ and $\bar{S}_{\min}^2$ is the average minimum of the residual dispersion. This ratio obeys the F-distribution (Eq. (A9)):

$$q(F_j) = \frac{\Gamma(\nu)/}{\Gamma^2(\nu/2)} \times \frac{F_j^{(\nu/2)-1}}{(1+F_j)^{\nu}} \tag{A9}$$

where n is the number of degrees of freedom equal for every dispersion and Γ is the Gamma function [27].

The probabilities of the jth function are computed on the assumption that the experimental data with L kinetic functions are described by a complete and independent events' systems (Eq. (A10))

$$\sum_{j=1}^{j=L} P_j = 1 \tag{A10}$$

Therefore we obtain (Eq. (A11))

$$P_j = \frac{Z_j}{\sum_{j=1}^{j=L} Z_j} \quad \text{with} \quad Z_j = 1 - \frac{\Gamma(\nu)}{\Gamma^2(\nu/2)} \int_0^{F_j} x^{(\nu/2)-1}(1+x)^{-\nu}\mathrm{d}x \tag{A11}$$